Acta Crystallographica Section D
Biological Crystallography
ISSN 0907-4449

A novel mechanism of sulfur transfer catalyzed by *O*-acetylhomoserine sulfhydrylase in the methionine-biosynthetic pathway of *Wolinella succinogenes*

Timothy H. Tran,[a] Kalyanaraman Krishnamoorthy,[b] Tadhg P. Begley[b]* and Steven E. Ealick[a]*

[a]Department of Chemistry and Chemical Biology, Cornell University, Ithaca, New York 14853-1301, USA, and [b]Department of Chemistry, Texas A&M University, College Station, TX 77842, USA

Correspondence e-mail: begley@tamu.edu, see3@cornell.edu

Received 10 May 2011
Accepted 12 July 2011

PDB Reference: MetY, 3ri6.

O-Acetylhomoserine sulfhydrylase (OAHS) is a pyridoxal 5′-phosphate (PLP) dependent sulfide-utilizing enzyme in the L-cysteine and L-methionine biosynthetic pathways of various enteric bacteria and fungi. OAHS catalyzes the conversion of *O*-acetylhomoserine to homocysteine using sulfide in a process known as direct sulfhydrylation. However, the source of the sulfur has not been identified and no structures of OAHS have been reported in the literature. Here, the crystal structure of *Wolinella succinogenes* OAHS (MetY) determined at 2.2 Å resolution is reported. MetY crystallized in space group *C*2 with two monomers in the asymmetric unit. Size-exclusion chromatography, dynamic light scattering and crystal packing indicate that the biological unit is a tetramer in solution. This is further supported by the crystal structure, in which a tetramer is formed using a combination of non-crystallographic and crystallographic twofold axes. A search for structurally homologous proteins revealed that MetY has the same fold as cystathionine γ-lyase and methionine γ-lyase. The active sites of these enzymes, which are also PLP-dependent, share a high degree of structural similarity, suggesting that MetY belongs to the γ-elimination subclass of the Cys/Met metabolism PLP-dependent family of enzymes. The structure of MetY, together with biochemical data, provides insight into the mechanism of sulfur transfer to a small molecule *via* a protein thiocarboxylate intermediate.

1. Introduction

Wolinella succinogenes is a Gram-positive bacterium that was originally found in cattle rumen. A member of the Helicobacteraceae group of ε-proteobacteria, *W. succinogenes* is a close relative of *Helicobacter pylori* and *Campylobacter jejuni*, which are known pathogens in humans and animals. Specifically, *H. pylori* has been linked to ulcers and gastric cancer and *C. jejuni* is known to cause Guillain–Barre syndrome (Mileni *et al.*, 2006).

O-Acetylhomoserine sulfhydrylase (OAHS; EC 4.2.99.10) is a sulfide-utilizing enzyme in the L-cysteine and L-methionine biosynthetic pathways employed by various enteric bacteria and fungi. OAHS is known to catalyze the conversion of *O*-acetylhomoserine (OAH) to homocysteine (Hcy) using sulfide directly (Yamagata, 1989). Recent biochemical studies (Krishnamoorthy & Begley, 2011) have suggested that the likely sulfur source in the methionine-biosynthetic pathway of *W. succinogenes* is a protein thiocarboxylate (Fig. 1). The pathway was identified from a gene cluster encoding a putative sulfur-carrier protein (HcyS), a putative metalloprotease

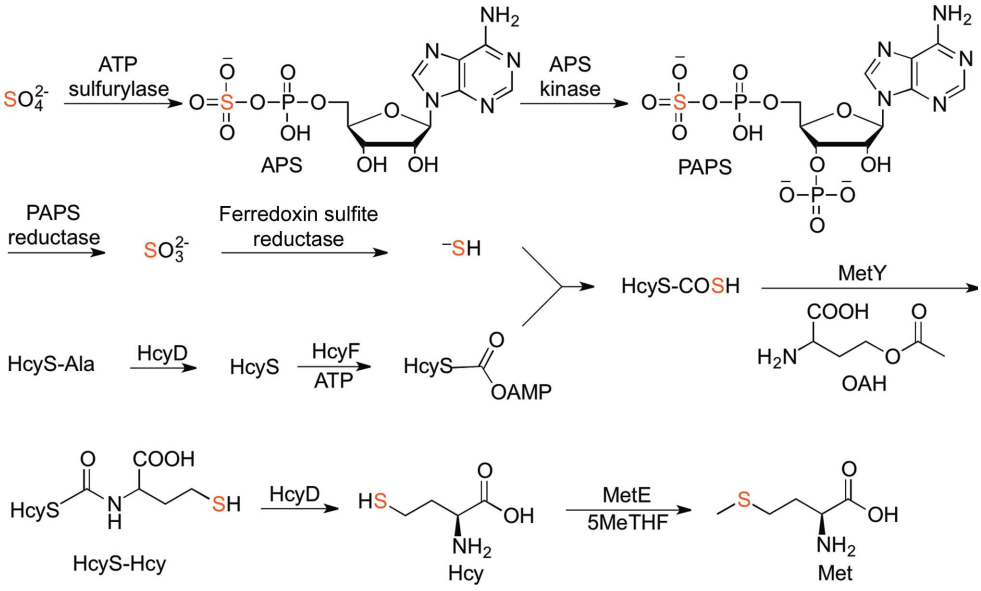

Figure 1
Proposed pathway for sulfur assimilation in *W. succinogenes*. MetY catalyses the PLP-dependent condensation of HcyS-COSH and OAH to form HcyS-Hcy. The S atom that originates from sulfate is highlighted in red throughout.

(HcyD), an adenylating enzyme (HcyF), sulfur-assimilating proteins and proteins for methionine biosynthesis found in this species. In this proposed pathway, sulfate is converted to adenosine 5′-phosphosulfate (APS), which is then phosphorylated at the 3′-hydroxyl group. The resulting 3′-phosphoadenosine 5′-phosphosulfate (PAPS) is reduced in two steps to sulfide, which is transferred to the C-terminal carboxylate of HcyS to form HcyS thiocarboxylate (HcyS-COSH). MetY then catalyzes the pyridoxal 5′-phosphate (PLP) dependent condensation of HcyS-COSH and OAH, followed by an *S*,*N*-acyl shift, to form HcyS-homocysteine (HcyS-Hcy), which is cleaved by HcyD to form homocysteine (Hcy). Finally, methylation of Hcy by MetE using 5-methyltetrahydrofolate (5MeTHF) as the cofactor produces methionine. Thus, the S atom of methionine originates from sulfate and is incorporated by MetY using the sulfur-carrier protein HcyS rather than directly from sulfide as is the case for other OAHSs (Yamagata, 1989).

Sulfur-carrier proteins have been implicated in several biosynthetic pathways, including those for thiamin (ThiS; Dorrestein *et al.*, 2004), molybdopterin (MoaD; Leimkühler *et al.*, 2001), cysteine (CysO; Burns *et al.*, 2005), thioquinolobactin (QbsE; Godert *et al.*, 2007), 2-thioribothymidine (TtuB; Shigi *et al.*, 2008) and 5-methoxycarbonylmethyl-2-thiouridine (Urm1p; Leidel *et al.*, 2009). In general, sulfur-carrier proteins are of low molecular weight (<10 000 Da) with a Gly-Gly C-terminus and have a ubiquitin-like fold. In some cases, such as HcyS and QbsE, the Gly-Gly motif may be followed by one or more additional amino-acid residues which must be cleaved before activation. The C-terminus of the sulfur-carrier protein is activated by adenylation and subsequently converted to the thiocarboxylate, which serves as the sulfur source for subsequent reactions.

In this study, we report the 2.2 Å resolution structure of MetY, the first documented OAHS for which the S atom is provided by the thiocarboxylate of a sulfur-carrier protein. By comparing this structure with those of other proteins, we found that MetY has the same fold as *Saccharomyces cerevisiae* cystathionine γ-lyase (ScCGL; PDB entry 1n8p; Messerschmidt *et al.*, 2003) and *Pseudomonas putida* methionine γ-lyase (PpMGL; PDB entry 2o7c; Kudou *et al.*, 2007). The structural similarity and active-site conservation suggest that MetY belongs to the Cys/Met metabolism PLP-dependent family of enzymes (PF01053; Bateman *et al.*, 2002), which catalyze a variety of reactions including γ-replacements, γ-eliminations and β-eliminations (Messerschmidt *et al.*, 2003). The structure described in this study, together with published biochemical data (Krishnamoorthy & Begley, 2011), results in the assignment of MetY as a γ-elimination enzyme and allows us to propose a mechanism for the protein thiocarboxylate-dependent sulfur-transfer reaction.

2. Experimental procedures

The cloning, overexpression, purification and assay of MetY have been described previously (Krishnamoorthy & Begley, 2011).

2.1. Crystallization

The frozen protein was thawed at 277 K. Crystallization of MetY was carried out by the hanging-drop vapor-diffusion method at 295 K using sparse-matrix screening solutions from Hampton Research and Emerald BioSystems. 1.5 µl protein solution was combined with an equal volume of well solution. Extensive screenings led to one condition consisting of 25–30%(*w*/*v*) ethylene glycol with 5%(*v*/*v*) *N*-dodecyl-*N*,*N*-dimethylamine-*N*-oxide detergent as an additive. The crystals grew as small blocks ranging from 25 to 50 µm in two of the dimensions and from 50 to 75 µm in the third dimension. The crystals used for X-ray diffraction experiments took approximately three months to grow.

2.2. Data collection and processing

Because of the relatively high concentration of ethylene glycol (25–30%) in the crystallization condition, no additional cryoprotection was required prior to data collection. X-ray diffraction data were collected from crystals of MetY on the

Table 1
Data-collection statistics.

Values in parentheses are for the highest resolution shell.

Beamline	F1, CHESS
Wavelength (Å)	0.916
Resolution (Å)	50–2.2
Space group	*C*2
Molecules per asymmetric unit	2
Unit-cell parameters	
a (Å)	161.8
b (Å)	62.5
c (Å)	91.6
α (°)	90.0
β (°)	120.5
γ (°)	90.0
Measured reflections	89132
Unique reflections	37506 (1862)
$\langle I/\sigma(I)\rangle$	11.0 (2.9)
Multiplicity	2.4 (2.3)
Completeness (%)	96.6 (98.2)
$R_{\rm merge}$† (%)	12.3 (40.1)

† $R_{\rm merge} = \sum_{hkl}\sum_i |I_i(hkl) - \langle I(hkl)\rangle| / \sum_{hkl}\sum_i I_i(hkl)$, where $\langle I(hkl)\rangle$ is the mean intensity of the *i* reflections with intensities $I_i(hkl)$ and common indices *hkl*.

F1 beamline outfitted with capillary focusing optics at the Cornell High Energy Synchrotron Source (CHESS) using an Area Detector System Corporation Quantum 270 detector. The data were collected using a wavelength of 0.916 Å over 360° with a 1° oscillation range. The data set was indexed, integrated and scaled using the *HKL*-2000 program suite (Otwinowski & Minor, 1997). Data-collection statistics are shown in Table 1.

2.3. Structure determination

The MetY structure was determined by molecular replacement using *MOLREP* (Vagin & Teplyakov, 2000) with the *Thermus thermophilus O*-acetylhomoserine sulfhydrylase (TtOAHS) structure (PDB entry 2cb1; T. Imagawa, H. Utsunomiya, Y. Agari, S. Satoh & H. Tsuge, unpublished work) as the search model. *CHAINSAW* (Schwarzenbacher *et al.*, 2004) was used to remove atoms that were not common to the two sequences. Refinement was performed using

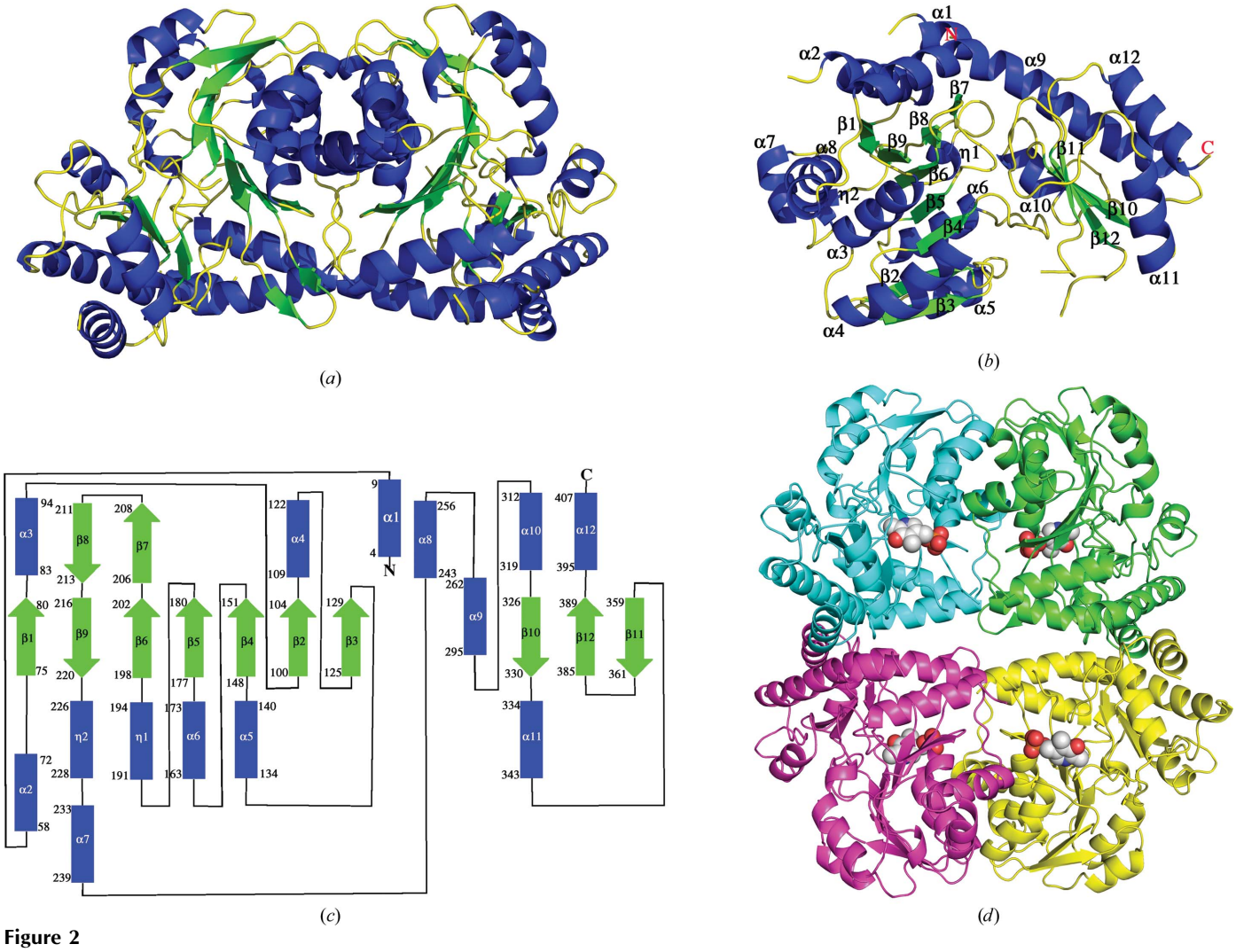

Figure 2
Structure of MetY. (*a*) Dimer observed in the asymmetric unit. (*b*) Monomer with secondary-structure elements labelled. (*c*) Topology diagram with the same labels as in (*b*). The numbers for the first and last amino-acid residue in each secondary-structure element are shown. (*d*) The biological tetramer. PLP is represented as spheres. The letters N and C in the monomer and topology diagrams denote the N- and C-termini, respectively.

Table 2
Data-refinement statistics.

Resolution (Å)	79–2.2
No. of protein atoms	5266
No. of water atoms	183
Reflections in working set	38264
Reflections in test set	2017
R factor† (%)	22.5
R_{free}‡ (%)	25.1
R.m.s.d. from ideals	
Bond lengths (Å)	0.024
Angles (°)	1.942
Average *B* factor (Å^2)	23.6
Ramachandran plot	
Most favored (%)	98.4
Additionally allowed (%)	1.6
Generously allowed (%)	0.0
Disallowed (%)	0.0

† R factor = $\sum_{hkl} ||F_{obs}| - |F_{calc}|| / \sum_{hkl} |F_{obs}|$, where F_{obs} and F_{calc} are observed and calculated structure factors, respectively. ‡ For R_{free}, the sum is extended over a subset of reflections (5%) excluded from all stages of refinement.

REFMAC (Murshudov *et al.*, 1999) and alternated with successive manual model building using *Coot* (Emsley & Cowtan, 2004) guided by an $F_o - F_c$ map, a $2F_o - F_c$ map and composite OMIT electron-density maps generated using *CNS* and *CCP*4 (Brünger *et al.*, 1998; Winn *et al.*, 2011). Water molecules were added after the *R* factor and R_{free} converged. The geometry of MetY was validated using *PROCHECK* (Laskowski *et al.*, 1993). Refinement statistics are summarized in Table 2.

2.4. Figure production

All figures were produced using *PyMOL* (DeLano, 2002), *ALSCRIPT* (Barton, 1993) and *ChemBioDraw* (CambridgeSoft).

3. Results

3.1. Structure of the MetY monomer

The Matthews coefficient (Matthews, 1968) for the MetY crystals was calculated to be 2.23 Å^3 Da^{-1}, which assuming two monomers per asymmetric unit corresponds to a solvent content of 45%. The final model (Fig. 2*a*), including two monomers and 183 water molecules, had an *R* factor and R_{free} of 22.5% and 25.1%, respectively. Of 407 possible amino-acid residues, monomer *A* contains residues 2–12, 57–367 and 377–407 and monomer *B* contains residues 2–11, 57–207, 211–364 and 381–406. Each monomer contains one active site. The monomer adopts an α/β fold and consists of a large central seven-stranded β-sheet, a two-stranded β-sheet and a three-stranded β-sheet. The β-sheets are flanked by a total of 12 α-helices and two 3_{10}-helices (Figs. 2*b* and 2*c*).

The electron density for two large segments was absent in both chains in the asymmetric unit. The longer segment is located at the N-terminus and consists of 44 residues (13–56) in monomer *A* and 45 residues (12–56) in monomer *B*, while the smaller segment is near the C-terminus and consists of nine residues (368–376) in monomer *A* and 16 residues (365–380) in monomer *B*. For both segments, electron density for the residues adjacent to the disordered loops (including the N-terminal helix α1) was clear, demonstrating that the protein was intact and not truncated. This is consistent with SDS–PAGE analysis, which showed that the molecular weight of the protein used for crystallization was near the expected value. The longer segment is also predicted to be involved in PLP binding (see below) and is most likely to be disordered because PLP is not bound in the crystal structure.

The monomer is composed of two domains. The large domain contains the PLP-binding site and the seven-stranded β-sheet, which is flanked by α2, α3, α4, α5, α6, α7, α8, η1, η2 and part of α9. The seven-

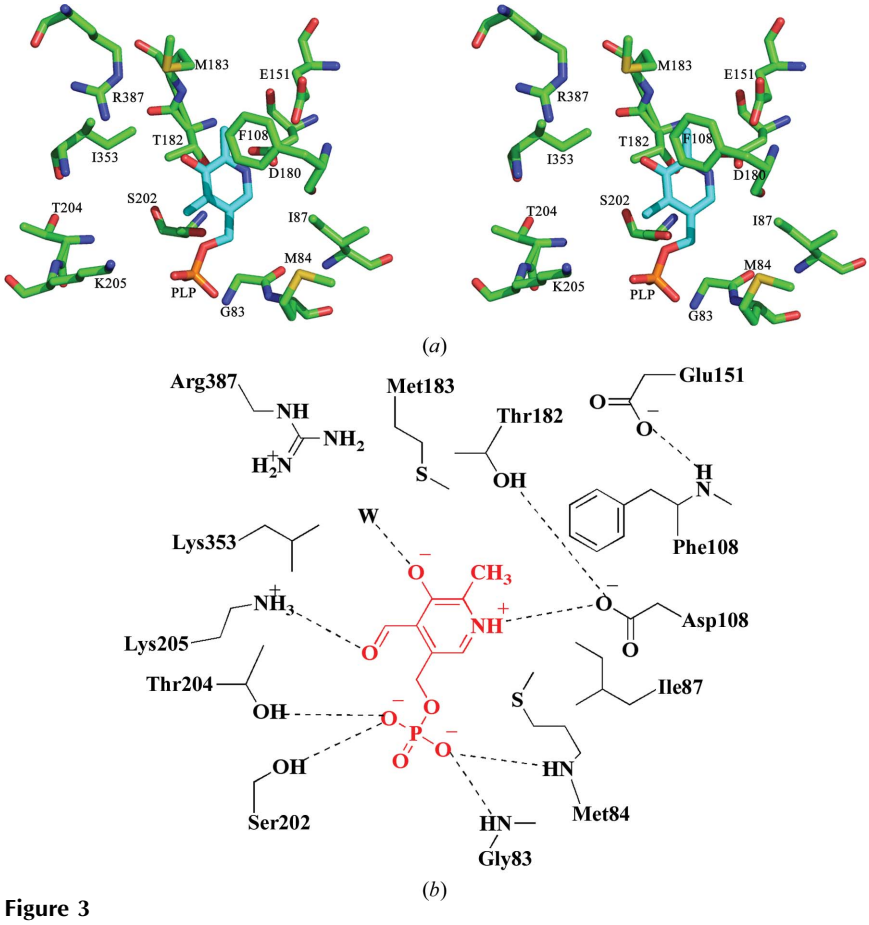

Figure 3
Model of the active site of MetY. (*a*) Stereo diagram. (*b*) Schematic representation. The PLP cofactor shown in cyan and red in (*a*) and (*b*), respectively, is manually positioned in the active site based on superposition of structural homologs. Predicted interactions are indicated by the dashed lines. 'W' denotes a water molecule.

Table 3
Enzymes structurally similar to MetY from *DALI*.

Protein	PDB code	*Z* score	R.m.s.d. (Å)	Identity (%)	No. of aligned residues	No. of residues
TtOAHS	2cb1	45.4	1.7	41	344	421
ScCGL	1n8p	41.9	1.5	33	322	368
PpMGL	1gc2	41.9	1.8	38	325	370

stranded β-sheet consists of mostly parallel strands with a strand order of $\beta1\uparrow\beta9\downarrow\beta6\uparrow\beta5\uparrow\beta4\uparrow\beta2\uparrow\beta3\uparrow$. The smaller domain, or the capping domain, resides near the C-terminal end and contains a slightly twisted antiparallel three-stranded β-sheet which is flanked by $\alpha9$, $\alpha10$, $\alpha11$ and $\alpha12$. $\beta7$ and $\beta8$ are continuous with $\beta6$ and $\beta9$, respectively, and extend to form another small β-sheet. Helix $\alpha9$ is unusually long, consisting of 34 residues and spanning the two domains. The compact monomer is achieved by the tight packing between the two domains.

3.2. Structure of the MetY tetramer

The two monomers in the asymmetric unit are related by noncrystallographic twofold symmetry (Fig. 2*a*) and a homotetramer with 222 symmetry is generated by the addition of a crystallographic twofold axis (Fig. 2*d*). This tetramer was confirmed as the biological unit of MetY based on size-exclusion chromatography and dynamic light scattering (data not shown). The dimensions of the monomer are approximately 50 × 50 × 70 Å and those of the tetramer are approximately 75 × 85 × 95 Å. The monomers are arranged such that the two active sites of any pair of adjacent monomers face in opposite directions. In this arrangement, adjacent monomers are closely packed with 1018 Å^2 of buried surface area per monomer as calculated by the *PISA* server (Krissinel & Henrick, 2005); however, diagonal monomers of the tetramer do not interact. Tightly packed monomers interact primarily *via* a long loop, $\alpha3$, $\alpha4$ and $\alpha8$. The active sites of the two closest monomers are about 20 Å apart and the active sites of the farthest monomers are 37 Å apart.

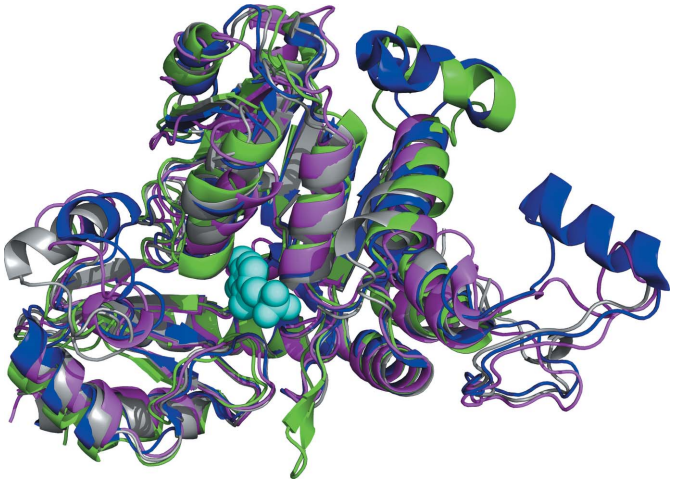

Figure 4
Structural superposition of the MetY monomer with homologous enzymes. Color coding is as follows: MetY, green; TtOAHS (PDB entry 2cb1), blue; ScCGL (PDB entry 1n8p), magenta; PpMGL (PDB entry 2o7c), gray. The PLP molecule is shown as cyan spheres.

3.3. MetY active site

Each monomer contains one PLP-binding site; however, the cofactor was not bound in the crystallized MetY. The putative active site was easily identified based on structural homology to PpMGL (PDB entry 2o7c; Kudou *et al.*, 2007) and ScCGL (PDB entry 1n8p; Messerschmidt *et al.*, 2003) and PLP was modeled into the active site. A stereo figure and schematic illustration of the active site are shown in Fig. 3. The active site appears as a relatively large cavity open to solvent. The active site is located near the N-terminus of $\alpha3$. The PLP-binding site is occupied by water molecules in the absence of the cofactor. On the basis of the model, the phosphate group of PLP makes hydrogen bonds to Thr204, Ser202 and the amide N atoms of Gly83 and Met84. Asp180 is within salt-bridge distance of the N1 atom of PLP. Leu353, Met183, Ile87 and Met84 interact with the hydrophobic region of PLP. Glu151 does not appear to interact directly with PLP, but could form a hydrogen bond to Phe108, which could stabilize the pyridine ring of PLP by a stacking interaction. Thr182 and Ser202 are about 3 Å directly below the plane of the pyridine ring of PLP according to the orientation shown in Fig. 3. In addition, Thr182 is also within hydrogen-bonding distance of Asp180. No residues in the active site appear to interact with the methyl group of PLP. The hydroxyl group of PLP could hydrogen bond to an ordered water molecule as seen in the structures of the homologs. With the exception of two PLP-binding residues from the disordered N-terminal loop, all of the residues that potentially interact with PLP originate from the large PLP-binding domain.

4. Discussion

4.1. Comparison of MetY to homologous enzymes

Although the asymmetric unit contains a dimer, the tetramer can be generated from the dimer using a crystallographic twofold axis. The tetrameric structure (Fig. 2) was supported by a *PISA* server analysis (Krissinel & Henrick, 2005) and experimentally by gel-filtration and dynamic light-scattering analysis. Furthermore, OAHS from *Schizosaccharomyces pombe* has been biochemically demonstrated to be tetrameric (Yamagata, 1984). The γ-lyases PpMGL and ScCGL also function biologically as tetramers (Kudou *et al.*, 2007; Messerschmidt *et al.*, 2003; Motoshima *et al.*, 2000; Nikulin *et al.*, 2008). In addition, the MetY tetramer is structurally homologous to those of PpMGL, ScCGL and TtOAHS.

The monomer contains two domains: a large PLP-binding domain and a small C-terminal domain. A search using the *DALI* server identified several structural homologs. The top representative hits are shown in Table 3 (Holm & Sander, 1998) and a superposition of the monomers from each structure with MetY is shown in Fig. 4. TtOAHS, which was the

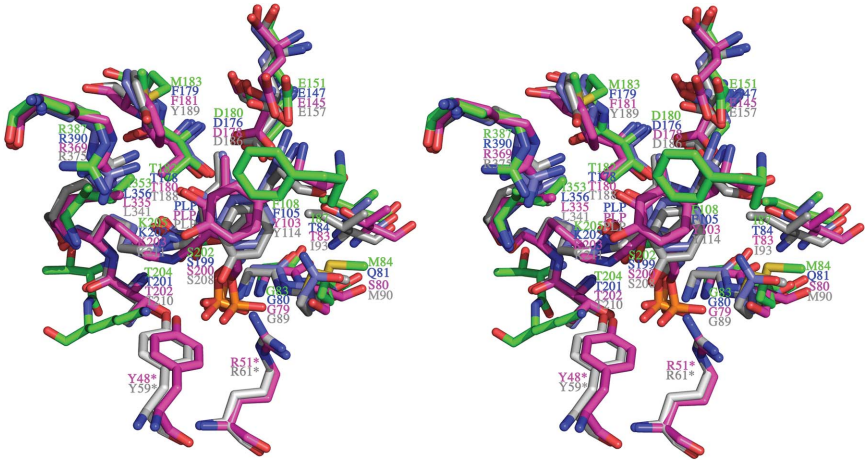

Figure 5
Superposition of the active sites of MetY with those of other γ-lyases. The enzymes and coloring schemes are the same as in Fig. 4, except that the color of PLP is the same as its corresponding enzyme. Residues marked with an asterisk are from a neighboring monomer.

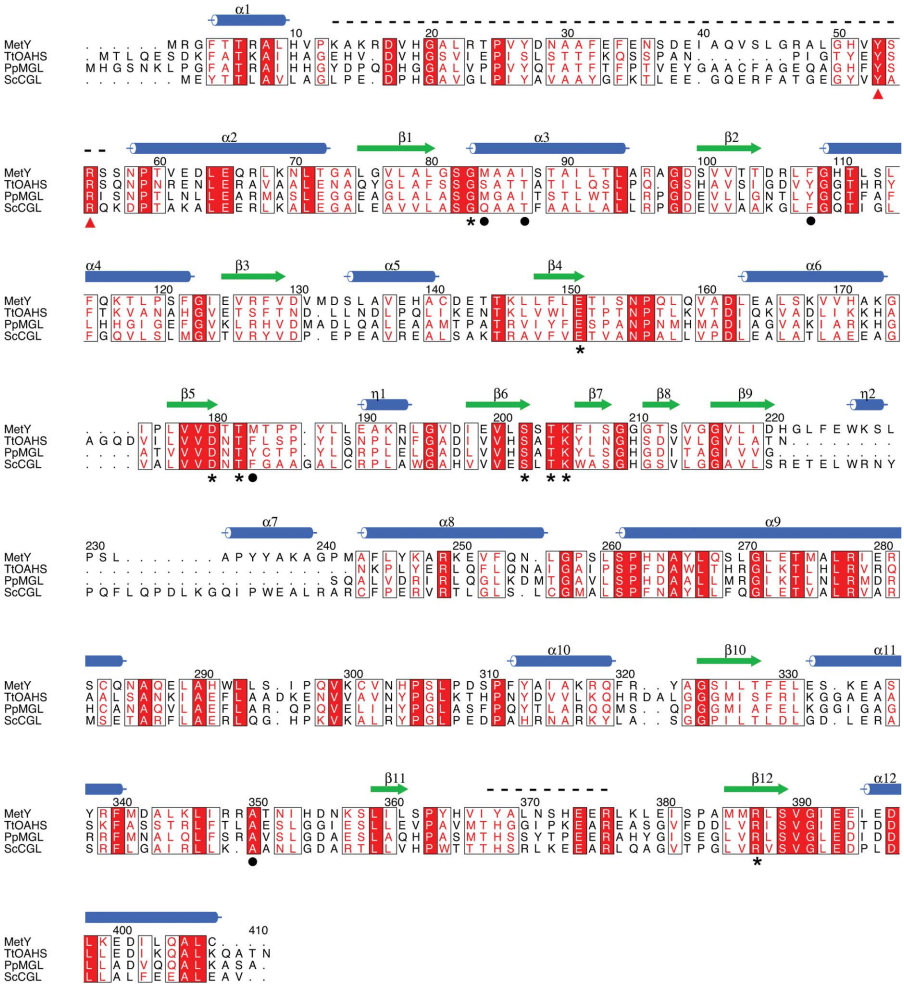

Figure 6
Sequence alignment of MetY with TtOAHS (PDB entry 2cb1), ScCGL (PDB entry 1n8p) and PpMGL (PDB entry 2o7c). Numbering and secondary-structure assignments are for MetY. Helices are indicated by blue cylinders, strands are indicated by green arrows and the two disordered loops are indicated by black dashed lines. Conserved residues are shown in boxes with white font and red shading. Conservative substitutions are shown in boxes with a red font. The conserved active-site residues are marked with asterisks and other active-site residues of MetY are marked with black circles. The two conserved residues from the disordered loop of an adjacent monomer, which are predicted to bind to the PLP phosphate group, are marked with red triangles.

search model for the molecular-replacement structure determination of MetY, was the top hit, with a Z score of 45.4 and an aligned sequence identity of 41%. The next two hits, ScCGL and PpMGL, with Z scores of 41.9, belong to the Cys/Met metabolism PLP-dependent family of enzymes (PF01053; Bateman *et al.*, 2002). This family of enzymes utilizes PLP to carry out β-eliminations, γ-eliminations and γ-replacements. Therefore, the *DALI* search results suggest that MetY may belong to the γ-elimination subfamily of the Cys/Met metabolism PLP-dependent family of enzymes.

The disordered N-terminal loop is located between helices α1 and α2. Both of these helices have well defined electron density in both monomers of MetY. In the structures of TtOAHS, PpMGL and ScCGL the corresponding loop is located at the monomer–monomer interface (Kudou *et al.*, 2007). Two absolutely conserved PLP-binding residues, corresponding to Tyr53 and Arg55 in MetY, are located near the end of the loop. These residues cap the PLP portion of the active site of the adjacent monomer. In the other structures both residues form hydrogen bonds to the PLP phosphate. Therefore, the absence of PLP in the MetY crystal structure is most likely to cause the loop to be disordered. The shorter disordered loop is located near the surface at an opening into the active site. In the structures of TtOAHS, PpMGL and ScCGL this region forms a short α-helix and caps the active site. It is likely that in MetY this region becomes ordered when substrate binds or that it mediates protein–protein interactions in the complex with HcyS-COSH.

4.2. Comparison of active sites for enzymes similar to MetY

Because MetY, TtOAHS, PpMGL and ScCGL are members of the same superfamily and share the same fold, we compared their active sites. The superposition of the active sites (Fig. 5, Table 4) of these homologs and MetY confirmed the location of the active site of MetY and showed highly conserved amino-acid residues. In addition to

Table 4
Comparison of active-site residues of different structural homologs of MetY.

PpMGL	ScCGL	MetY	TtOAHS	Predicted role in MetY
Gly89	Gly79	Gly83	Gly80	Amide hydrogen interacts with the phosphate group of PLP
Met90	Ser80	Met84	Gln81	Interacts hydrophobically with PLP ring and its amide hydrogen makes a hydrogen bond with the phosphate group of PLP
Ile93	Thr83	Ile87	Thr84	Interacts with the hydrophobic part of PLP ring
Tyr114	Tyr103	Phe108	Phe105	Stabilizes the pyridine ring of PLP by π-stacking interaction
Glu157	Glu145	Glu151	Glu147	Positions Phe108 in the active site
Asp186	Asp178	Asp180	Asp176	Forms a salt bridge with the N1H atom of PLP
Thr188	Thr180	Thr182	Thr178	Makes van der Waals interaction and a hydrogen bond with the π-electron ring of PLP
Tyr189	Phe181	Met183	Phe179	Interacts with the hydrophobic part of PLP ring
Ser208	Ser200	Ser202	Ser199	Makes van der Waals interaction with the π-electron ring and a hydrogen bond with the phosphate group of PLP
Thr210	Thr202	Thr204	Thr201	Hydrogen bonds with the phosphate group of PLP
Lys211	Lys203	Lys205	Lys202	Makes a Schiff-base linkage with PLP
Leu341	Leu335	Ile353	Leu356	Interacts with the hydrophobic part of the PLP ring
Arg375	Arg369	Arg387	Arg390	Interacts with the carboxylate group of *O*-acetylhomoserine
Tyr59†	Tyr48†	Tyr50†	Tyr53†	Hydrogen bonds with the phosphate group of PLP
Arg61†	Arg51†	Arg52†	Arg55†	Hydrogen bonds with the phosphate group of PLP

† Residues from the adjacent dimer of the active monomer.

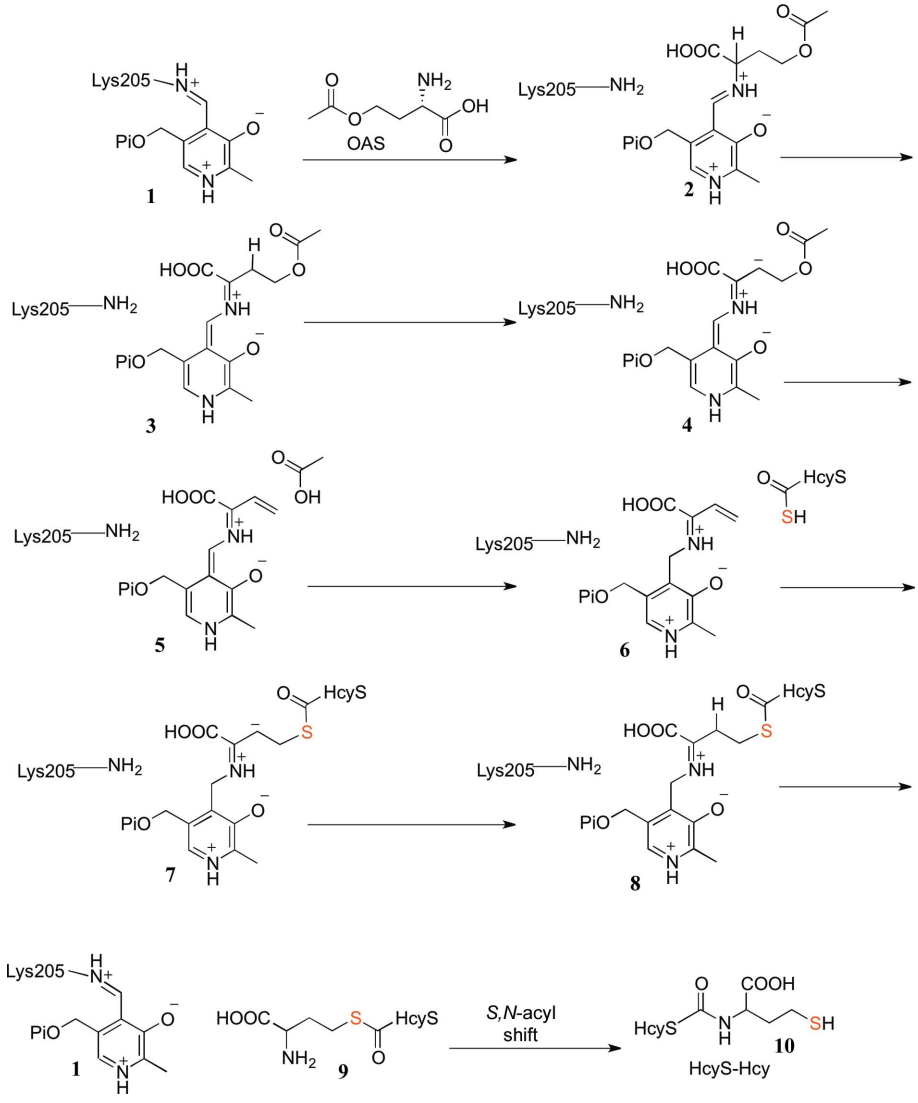

Figure 7
Mechanistic proposal for MetY-catalyzed sulfur transfer from HcyS-COSH to OAH. The S atom that originates from sulfate is highlighted in red.

the biochemical data, which show that MetY requires PLP for activity, MetY appeared yellow throughout the purification procedure, suggesting the presence of PLP, despite its absence in the crystal structure. By comparing the active-site residues of MetY with those of TtOAHS (PDB entry 2cb1; T. Imagawa, H. Utsunomiya, Y. Agari, S. Satoh & H. Tsuge, unpublished work), PpMGL (Kudou *et al.*, 2007) and ScCGL (Messerschmidt *et al.*, 2003), the critical active-site residues were identified. A sequence alignment with these residues identified is shown in Fig. 6. The equivalent residues to Phe108 of MetY in the other three structures form π-stacking interactions with the pyridine ring of PLP (Clausen *et al.*, 1998; Hayashi *et al.*, 1990), suggesting that Phe108 plays the same role in MetY. The conserved Glu151 does not interact directly with PLP, but is positioned to form a hydrogen bond to the backbone amide of the active-site residue Phe108. In the absence of PLP, Phe108 is rotated slightly away from where PLP is postulated to bind. The conserved residues Thr182 and Ser202 may form van der Waals interactions with the pyridine ring of PLP as well as forming electrostatic interactions with the π-electron ring. Together with Phe108, Thr182 and Ser202 sandwich PLP in the active site. Thr182 also hydrogen bonds to the amide H atom of the conserved Asp180 and positions it for a salt bridge to N1 of PLP. Lys205 is conserved within the superfamily and forms a Schiff-base linkage with PLP prior to substrate binding. In the MetY active site, Thr204 and Ser202 are predicted to form hydrogen bonds to the PLP phosphate group and are conserved. On the basis of comparison with the homologous structures, Phe108, Thr204 and Lys205 move away from the active site in the absence of PLP. The active site is accessible to solvent in the absence of PLP; however, ordering of the shorter disordered loop region would reduce active-site accessibility. The backbone amide groups of Met84 and the conserved Gly83 are in position to hydrogen bond to the phosphate group of PLP. The conserved Arg387 does not appear to make any contacts with PLP,

while its equivalents in PpMGL and ScCGL are known to bind to the carboxylate group of the incoming substrate (Kudou *et al.*, 2007; Messerschmidt *et al.*, 2003). Ile353, Met183, Ile87 and Met84 are in position to interact with the hydrophobic region of PLP.

4.3. Mechanistic implications

The primary sequence of MetY and its structural alignment with homologs suggest that MetY belongs to the Cys/Met metabolism PLP-dependent family of enzymes (PF01053; Bateman *et al.*, 2002). This family also includes CysM, which catalyzes the transfer of sulfur from CysO thiocarboxylate (CysO-COSH) to *O*-phosphoserine (OPS; Jurgenson *et al.*, 2008; O'Leary *et al.*, 2008). Our biochemical and structural data suggest that MetY-catalyzed sulfur transfer from HcyS-COSH to OAH is similar to the CysM-catalyzed sulfur transfer from CysO-COSH to OPS. A mechanistic proposal is outlined in Fig. 7. In this proposal, a transimination between **1** and OAH gives imine **2**. Deprotonation gives **3**. A second deprotonation gives the stabilized carbanion **4**, from which the acetyl group is eliminated to give **5**. By reversal of these steps, HcyS-COSH gives **8**. Product release by a transimination gives **9**, which then undergoes a spontaneous N/S acyl shift to give the HcyS-Hyc **10**. Our structure suggests that the active site of MetY is accessible to the C-terminus of HcyS-COSH, thus allowing the thiocarboylate to position itself for sulfur transfer.

4.4. Significance

The structural studies reported here demonstrate that MetY belongs to the γ-elimination subclass of the Cys/Met metabolism family of PLP-dependent enzymes (PF01053; Bateman *et al.*, 2002). This suggests that MetY catalyzes a γ-elimination reaction to produce Hcy that is covalently attached to the HcyS sulfur-carrier protein. Therefore, MetY is likely to be mechanistically similar to OAHS except that the sulfur donor is a protein thiocarboxylate rather than a sulfide. MetY is a member of a growing family of proteins involved in sulfur transfer from protein thiocarboxylates. Eight species identified to date in the SEED database (Overbeek *et al.*, 2005) contain a gene-clustering pattern in which a sulfur-carrier protein gene is clustered with genes for a sulfur-assimilation pathway and methionine biosynthesis.

We thank Dr Cynthia Kinsland of the Cornell University Protein Facility for cloning MetY and the MacCHESS staff, supported by NIH grant RR01646, at the Cornell High Energy Synchrotron Source for assistance during data collection. We thank Dr Michael Fenwick for performing the light-scattering experiments. We thank Ms Leslie Kinsland for her assistance during manuscript preparation. This work supported by NIH grant DK67081.

References

Barton, G. J. (1993). *Protein Eng.* **6**, 37–40.
Bateman, A., Birney, E., Cerruti, L., Durbin, R., Etwiller, L., Eddy, S. R., Griffiths-Jones, S., Howe, K. L., Marshall, M. & Sonnhammer, E. L. (2002). *Nucleic Acids Res.* **30**, 276–280.
Brünger, A. T., Adams, P. D., Clore, G. M., DeLano, W. L., Gros, P., Grosse-Kunstleve, R. W., Jiang, J.-S., Kuszewski, J., Nilges, M., Pannu, N. S., Read, R. J., Rice, L. M., Simonson, T. & Warren, G. L. (1998). *Acta Cryst.* D**54**, 905–921.
Burns, K. E., Baumgart, S., Dorrestein, P. C., Zhai, H., McLafferty, F. W. & Begley, T. P. (2005). *J. Am. Chem. Soc.* **127**, 11602–11603.
Clausen, T., Huber, R., Prade, L., Wahl, M. C. & Messerschmidt, A. (1998). *EMBO J.* **17**, 6827–6838.
DeLano, W. L. (2002). *PyMOL*. http://www.pymol.org.
Dorrestein, P. C., Zhai, H., McLafferty, F. W. & Begley, T. P. (2004). *Chem. Biol.* **11**, 1373–1381.
Emsley, P. & Cowtan, K. (2004). *Acta Cryst.* D**60**, 2126–2132.
Godert, A. M., Jin, M., McLafferty, F. W. & Begley, T. P. (2007). *J. Bacteriol.* **189**, 2941–2944.
Hayashi, H., Inoue, Y., Kuramitsu, S., Morino, Y. & Kagamiyama, H. (1990). *Biochem. Biophys. Res. Commun.* **167**, 407–412.
Holm, L. & Sander, C. (1998). *Nucleic Acids Res.* **26**, 316–319.
Jurgenson, C. T., Burns, K. E., Begley, T. P. & Ealick, S. E. (2008). *Biochemistry*, **47**, 10354–10364.
Krishnamoorthy, K. & Begley, T. P. (2011). *J. Am. Chem. Soc.* **133**, 379–386.
Krissinel, E. & Henrick, K. (2005). *CompLife 2005*, edited by M. R. Berthold, R. Glen, K. Diederichs, O. Kohlbacher & I. Fischer, pp. 163-174. Berlin, Heidelberg: Springer-Verlag.
Kudou, D., Misaki, S., Yamashita, M., Tamura, T., Takakura, T., Yoshioka, T., Yagi, S., Hoffman, R. M., Takimoto, A., Esaki, N. & Inagaki, K. (2007). *J. Biochem.* **141**, 535–544.
Laskowski, R. A., Moss, D. S. & Thornton, J. M. (1993). *J. Mol. Biol.* **231**, 1049–1067.
Leidel, S., Pedrioli, P. G., Bucher, T., Brost, R., Costanzo, M., Schmidt, A., Aebersold, R., Boone, C., Hofmann, K. & Peter, M. (2009). *Nature (London)*, **458**, 228–232.
Leimkühler, S., Wuebbens, M. M. & Rajagopalan, K. V. (2001). *J. Biol. Chem.* **276**, 34695–34701.
Matthews, B. W. (1968). *J. Mol. Biol.* **33**, 491–497.
Messerschmidt, A., Worbs, M., Steegborn, C., Wahl, M. C., Huber, R., Laber, B. & Clausen, T. (2003). *Biol. Chem.* **384**, 373–386.
Mileni, M., MacMillan, F., Tziatzios, C., Zwicker, K., Haas, A. H., Mäntele, W., Simon, J. & Lancaster, C. R. (2006). *Biochem. J.* **395**, 191–201.
Motoshima, H., Inagaki, K., Kumasaka, T., Furuichi, M., Inoue, H., Tamura, T., Esaki, N., Soda, K., Tanaka, N., Yamamoto, M. & Tanaka, H. (2000). *J. Biochem.* **128**, 349–354.
Murshudov, G. N., Vagin, A. A., Lebedev, A., Wilson, K. S. & Dodson, E. J. (1999). *Acta Cryst.* D**55**, 247–255.
Nikulin, A., Revtovich, S., Morozova, E., Nevskaya, N., Nikonov, S., Garber, M. & Demidkina, T. (2008). *Acta Cryst.* D**64**, 211–218.
O'Leary, S. E., Jurgenson, C. T., Ealick, S. E. & Begley, T. P. (2008). *Biochemistry*, **47**, 11606–11615.
Otwinowski, Z. & Minor, W. (1997). *Methods Enzymol.* **276**, 307–326.
Overbeek, R. *et al.* (2005). *Nucleic Acids Res.* **33**, 5691–5702.
Schwarzenbacher, R., Godzik, A., Grzechnik, S. K. & Jaroszewski, L. (2004). *Acta Cryst.* D**60**, 1229–1236.
Shigi, N., Sakaguchi, Y., Asai, S., Suzuki, T. & Watanabe, K. (2008). *EMBO J.* **27**, 3267–3278.
Vagin, A. & Teplyakov, A. (2000). *Acta Cryst.* D**56**, 1622–1624.
Winn, M. D. *et al.* (2011). *Acta Cryst.* D**67**, 235–242.
Yamagata, S. (1984). *J. Biochem.* **96**, 1511–1523.
Yamagata, S. (1989). *Biochimie*, **71**, 1125–1143.